A STUDY OF WIND SPEED MODIFICATION AND INTERNAL BOUNDARY-LAYER HEIGHTS IN A COASTAL REGION

HANS BERGSTRÖM, PER-ERIK JOHANSSON, and ANN-SOFI SMEDMAN

Department of Meteorology, Uppsala University, Box 516, S-751 20 Uppsala, Sweden

(Received in final form 22 July, 1987)

Abstract. Wind profile data within the first two kilometres of a coast have been used to study the wind field modification downstream of this surface discontinuity. The land area is generally very flat, having an overall roughness length of 0.04 m. A wind model, suitable for practical applications and inexpensive to run, has been tested against the data and was found to give satisfactory results. Knowing the climatological statistics of wind and stratification, e.g., at the coast, the model may thus be used to estimate, on a climatological basis, how the wind field is modified with distance inland, at least in areas with only minor topography. This type of information is of great importance when locating wind turbines. It is in these cases also important to know the statistics of the internal boundary-layer (IBL) height, as the turbulence intensity may be quite different in and above the IBL, which in turn may influence load and fatigue calculations. Using the wind profile data, the IBL height was clearly discernible in the majority of cases. Having very unstable stratification over land, the IBL height could, however, not be determined from the wind profiles, as the wind in these cases did not decrease inland. This result was also obtained using the wind model. A simple model of the type $z_{IBL} = a \cdot x^b$, was instead tested, and was shown to give reasonable results.

Notation

a, b	parameters in the expression for z_{IBL},
f	Coriolis parameter,
H	sensible heat flux,
k	von Kármán's constant,
K	eddy diffusivity for momentum,
L	Monin–Obukhov length,
u, v	wind components,
u_g, v_g	geostrophic wind components,
u_*	friction velocity,
U	horizontal wind speed,
$U(0, z)$	equilibrium wind profile upstream of a surface discontinuity,
$U(\infty, z)$	equilibrium wind profile downstream of a surface discontinuity,
x	horizontal downstream distance,
z	height,
z_{IBL}	height of the internal boundary layer,
θ	potential temperature,
θ_*	scaling temperature,
λ	wind model parameter,
σ_u	standard deviation of the longitudinal wind component,
ϕ_h	dimensionless potential temperature gradient,
ϕ_m	dimensionless wind gradient.

1. Introduction

During the period 28 July to 28 August, 1984, a comprehensive meteorological field experiment, NIBWAK (Näsudden Internal Boundary Layer and WAKe experiment),

Boundary-Layer Meteorology **42** (1988) 313–335.

was realized at the Näsudden peninsula on the island of Gotland in the Baltic Sea. The experiment was a co-operative one between the Departments of Meteorology at the Universities of Uppsala and Athens. The main object was to study, in as much detail as possible, the lower parts of the atmospheric boundary layer, up to a few hundred metres, especially the Internal Boundary Layer (IBL), the structure of the atmospheric turbulence, and the wake behind the 2 MW wind turbine situated on the peninsula.

In this paper, we shall report on the modification of wind speed and the growth of the IBL as determined from the wind profile, experienced when the air flow passes a coast-line after a long passage over the sea. Observations of IBLs of different scales have earlier been reported with fetches ranging from less than 1 m (Bradley, 1968) to about 30 km (Raynor, 1979). The majority of experiments are, however, made over relatively short fetches and with measurements in the surface layer alone, up to heights of about 10 m. The data from the NIBWAK experiment offer an opportunity to study the IBL over a distance of 1.5 km and up to heights of 100–150 m.

Although the IBL concept is somewhat artificial, it offers a simple method to visualize a phenomenon which occurs frequently in nature. Knowledge about the structure and height of the IBL is of great importance, for instance when locating wind turbines. It is important to know how the potential energy output depends upon the distance from the coast at different heights. Furthermore, the height of the IBL will be of interest when performing load and fatigue calculations, as the degree of turbulence will often be quite different in and above the IBL.

In this context, it is important also to be aware of how the IBL height has been defined because different definitions may give quite different results. As was shown in Ogawa and Ohara (1985), the height determined from the wind profile is lower than the one resulting from the temperature profile. Gamo *et al.* (1982) showed that when comparing IBL heights determined from temperature and turbulence, the latter gave higher values, while Smedman and Högström (1983) got a higher value from the temperature profile than from the profile of sensible heat flux. As the present study is confined to wind profiles, we may thus expect comparatively low values of the IBL heights.

There is, of course, a great need for models capable of describing the modification of the onshore air flow as a function of distance from the coastline. Measurements are only available from a few sites and they will at most give us a good sample of data. To be able to get information and climatological statistics at a specific location, a model of some kind has to be used. Models over a wide range of complexity have been presented in the literature, from very simple ones (Elliott, 1958; Pasquill, 1972; Smedman and Högström, 1978) to the more complex higher order closure models (Peterson, 1969; Mellor and Yamada, 1974; André *et al.*, 1978; Enger, 1985). We have chosen to use a model of moderate complexity (Bergström, 1986), suitable for practical applications and easy to use. Simulating the wind profiles at different distances from the coast, the modification of the wind field downstream of a discontinuity, and its dependence on stability (upstream as well as downstream) and surface roughness change, may be illustrated.

As will be shown, it is not possible, however, to determine the height of the IBL from the wind model simulations (or from wind profile observations) in all cases. Instead,

a model of the type $z_{IBL} = a \cdot x^b$ has been adjusted to our data, keeping the parameter a constant and allowing b to vary with stability.

2. Site and Data

The experimental site at the Näsudden peninsula on the southwestern coast of the island of Gotland in the Baltic Sea, is generally very flat, covered mainly with farmland and areas with scattered juniper bushes and only a few trees. In the direction used in the IBL study, the terrain rises smoothly from sea level to 5 m over a distance of 1.5 km.

The measurements were made using 6 types of measuring systems: slow- and fast-response instruments in towers, tethered balloon soundings, radiosoundings, SODAR-measurements, and pibal trackings. The different systems were arranged in such a way that the IBL could be studied at various distances from the coastline; see Figure 1. The principles of the measuring systems are briefly outlined below.

Profile measurements on towers:

Slow-response instrumentation was installed on two towers at position 3 (cf. Figure 1), with measurements at 10 levels from 2 to 138 m. At position 1, a telescopic mast was

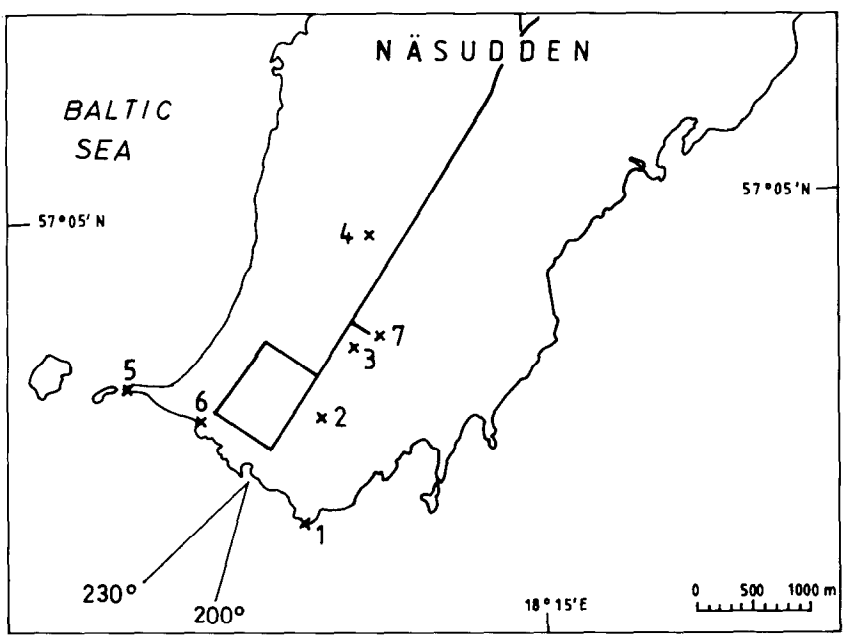

Fig. 1. Map of the Näsudden peninsula, showing the measurement sites: (1) 25 m mast, (Österudd); (2) tethered balloon soundings, ca. 800 m from the shore; (3) 145 m + 12 m mast ca. 1500 m from the shore; (4) SODAR ca. 2300 m from the shore; (5) theodolite site where pilot balloons were released; (6) theodolite site; (7) wind turbine. The wind direction interval (200–230°) accepted is also included in the figure.

erected with measurements at 4 levels from 2 to 16 m. The purpose was to get upstream profiles and the mast was placed right at the water's edge.

The wind speed was measured with cup-anemometers of the Casella and Teledyne types; potentiometer wind-vanes were used to obtain wind direction. The temperature was measured with ventilated and radiation shielded resistance thermometers (Pt-500). Details of the profile measuring system are given in Högström *et al.* (1978).

Turbulence measurements:

Meaurements of the turbulent fluctuations of wind and temperature were made at position 3 at three levels, 11, 77, and 135 m. The instrument was a wind-vane based three-component hot-wire system (Högström *et al.*, 1980; Högström, 1982). During situations judged to be of special interest, data were sampled at 20 Hz; otherwise the sampling frequency was set at 1 Hz.

Tethered balloon soundings:

These soundings were performed at location 2 (Figure 1) when the wind direction was favourable for IBL studies. The sounding system was designed at the Department of Meteorology in Uppsala and measures pressure, temperature, humidity, wind speed and direction (Smedman and Melas, 1986; Smedman and Lundin, 1987). The measured values are transmitted to a ground receiver and evaluated on line with a micro computer. Some caution is required when analysing sounding data, as this system, unlike the tower measurements, does not give simultaneous data from all levels. A complete sounding, up and down, lasts about 2 hours.

Sodar-measurements:

A three-axis Doppler sodar system, manufactured by Sensitron AB in Sweden, (cf. Salomonsson, 1982), was continuously in operation at location 4. The maximum measuring height is highly variable, as it requires temperature fluctuations in the atmosphere. For our data, the maximum heights were usually between 200 and 400 m.

Radio-soundings:

These were made with a radio-sonde of the Vaisala-type (RS-80), one or a few times per day during periods of special interest.

Pibal measurements:

During periods with intense IBL studies, double theodolite pilot balloon trackings were made from positions 5 (balloon release place) and 6. The technique is described in detail by Alexandersson and Bergström (1979). Measurements were made up to a height of about 2000 m; as the balloons were released at the shoreline, the profiles represent the conditions over the sea.

The weather conditions during IBL experiments were generally influenced by high pressure areas; only occasionally did low pressure systems, with accompanying fronts

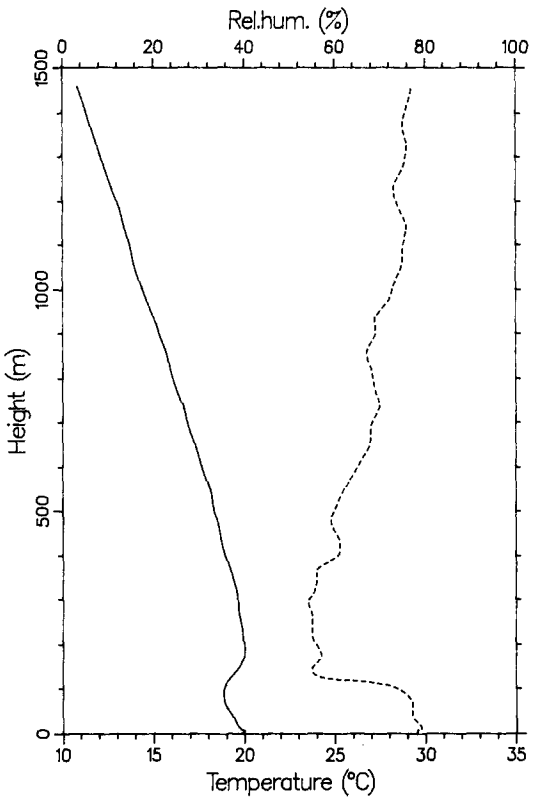

Fig. 2. Profiles of temperature (full line) and relative humidity (dashed line) from the radiosonde released 24 August, 1984 10.14 h at position 5 (cf. Figure 1).

and rain, pass the Gotland region. Within the high pressure systems, a subsidence inversion was often found at rather low levels over the Baltic Sea, usually in the height interval 100–300 m.

An example of this is given in Figure 2, which shows profiles of temperature and relative humidity as measured by the radiosonde system. Here the inversion began already at about 100 m, which is low enough to complicate the IBL studies. Often a wind maximum was found in the inversion layer. This inversion also had a great influence upon the turbulence structure. Thus we found rather large counter-gradient fluxes of sensible heat at the 135 m level, especially on August 21st, cf. Table I, where $H_{135} = 94$ W m^{-2} at 13.20 h, although $\partial\theta/\partial z \approx 0.01$ K m^{-1}.

3. Observed IBL Characteristics

As we have seen from Figure 1, the measuring equipment was arranged so as to make the data suitable for IBL studies. Profiles were measured continuously on two towers, at the coast and 1500 m inland, while the sodar gave wind profiles 2300 m from the coast. Tethered balloon soundings were occasionally made at the distance 800 m. Some

TABLE I

Basic data from the 145 m tower for the periods used in the IBL study. U = mean wind speed at 9 m, σ_u = standard deviation of the longitudinal wind component, H = sensible heat flux, z/L = stability parameter (L = the Monin–Obukhov length)

Date	Time (UTC + 1h)	U (m s^{-1})	σ_u (m s^{-1})			H (W m^{-2})			z/L 11 m
			11 m	77 m	135 m	11 m	77 m	135 m	
840803	16.05	4.3	0.92	0.37	0.28	22	14	8	−0.133
	17.05	4.2	1.04	0.38	0.31	38	27	26	−0.255
840806	14.53	7.4	1.33	0.69	0.50	83	38	25	−0.048
	16.05	6.7	1.24	0.58	0.41	46	18	12	−0.035
	18.30	6.3	1.14	0.60	0.53	1	8	11	−0.001
	19.15	5.9	1.09	0.59	0.54	−8	4	6	0.011
	21.25	5.4	0.98	0.68	0.59	−18	1	5	0.032
840807	12.05	3.2	0.72	0.46	0.44	102	10	−8	−3.616
	13.00	2.9	0.77	0.40	0.38	88	−19	−12	−7.126
	16.15	3.0	0.79	0.38	0.32	42	−7	−31	−0.820
	17.00	2.8	0.81	0.38	0.29	27	−14	−32	−0.711
840819	13.50	6.2	0.97	0.59	0.38	105	64	27	−0.173
	20.45	5.5	0.97	0.47	0.34	−14	−0	−3	0.030
840821	13.20	4.2	0.71	0.53	0.48	111	77	94	−0.320
	16.50	3.9	0.62	0.42	0.35	39	13	5	−0.147
	17.35	4.0	0.57	0.45	0.33	14	10	−8	−0.138
	22.10	3.1	0.38	0.21	0.19	−8	1	−1	0.217
	22.50	3.2	–	–	–	–	–	–	–
840822	02.48	3.0	0.36	0.29	0.26	−8	1	−2	0.219
	08.20	5.5	0.90	0.52	0.32	80	47	15	−0.113

basic meteorological data from the periods chosen for the IBL studies are given in Table I. Only periods having tethered balloon soundings are included in the table and the wind direction interval accepted is between 200 and 230°. A total of 20 periods with a length of about 1 hour then remained for the IBL study. In this paper, we shall concentrate entirely on the wind data.

An example of the observed gradual wind profile modification is given in Figure 3, which shows the hourly mean wind profiles at position 1 and 3, together with the corresponding tethered balloon sounding and sodar data. Comparing the two tower profiles, we see that at position 3 (1500 m from the coast) the IBL has grown to about 50 m and the 10 m wind speed has decreased from 8 m s^{-1} to about 6.5 m s^{-1}. To be able to compare, in more detail, the wind profile from the tethered balloon system with the tower profiles, it was necessary to smooth the sounding data by adapting it to a second-order polynomial in log$z$. In this way, it was possible to identify the IBL height also at the distance 800 m, which in this case was found to be about 30 m.

The sodar data do not agree with the other observations, not even at heights where the wind should be unaffected by the IBL. Several reasons for this may be put forward. One is that the sodar data were sampled as hourly mean values, and thus the time factor enters as a source of error, as it is not possible to get profiles which are simultaneous

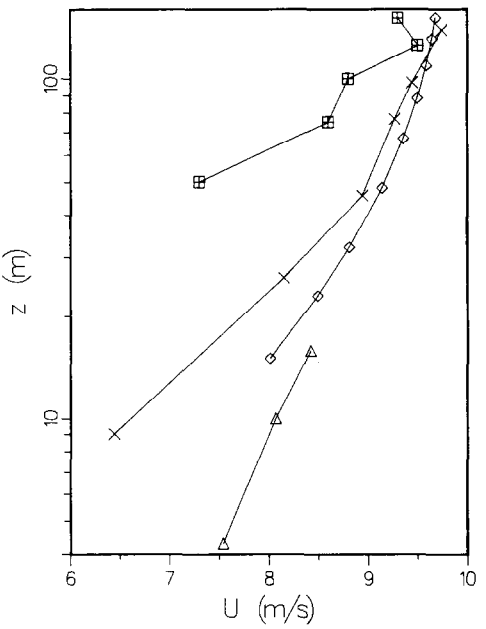

Fig. 3. Wind profiles 6 August, 1984 18.32 h, Δ at position 1 (cf. Figure 1), ◇ at position 2, × at position 3, ⊞ at position 4.

in time with the other data. Another source of uncertainty is the sodar technique itself. Comparisons between sodar and tower data often give satisfactory results, but from experience we know that the sodar technique is not always exact. Deviations of about 5% from the 'true' wind speed are not unusual. From a comparison with the tower data and the pibal data, we found that the sodar gave a mean wind speed which was about 0.4 m s^{-1} too low during this experiment. Applying a correction of this size to the sodar-profile in Figure 3, the agreement with the other data will be much better. A consequence of this rather small error is, however, that the sodar data are not accurate enough to be used to study the wind speed modification in the IBL.

Typical two-dimensional wind speed patterns are given in Figures 4 and 5, where lines with equal velocity are plotted versus height and distances from the coast. Observations from positions 1–5 were used when drawing the isolines and are included in the figures (marked with ×). In the example from daytime conditions (Figure 4), we see that the wind speed decreased about 0.5–1 m s^{-1} in the lower 50 m of the atmosphere, while higher up, the decrease was less than 0.5 m s^{-1}. During the night, when the stratification was stable, the wind speed decreased much more in the lower parts of the IBL. From the example given in Figure 5, we see that the wind speed in this case had decreased 2–2.5 m s^{-1} below 10 m height, while between 50 and 100 m, the decrease was only about 0.5 m s^{-1}.

The typical diurnal variation of the inland modification of the wind speed is illustrated in Figures 6 and 7. These figures show examples of the hourly mean wind profiles at

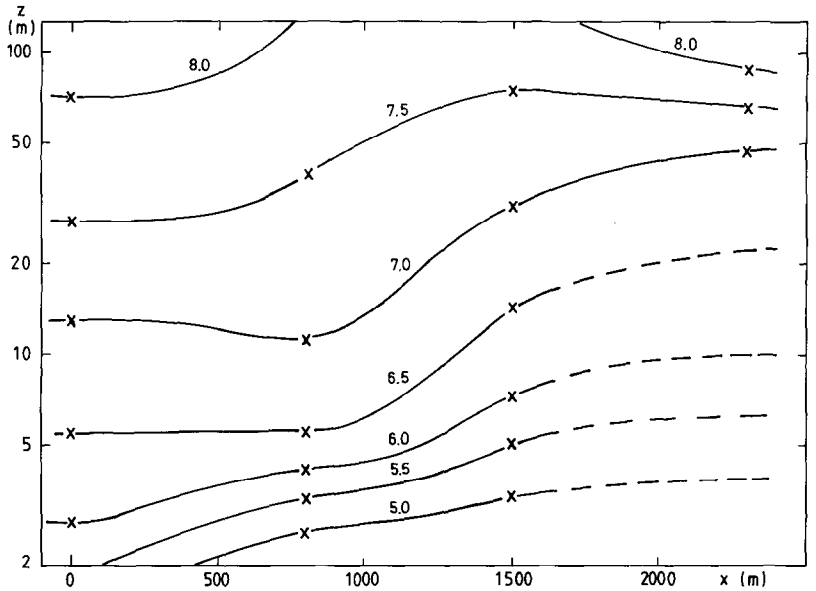

Fig. 4. The observed wind velocity field (m/s) versus height and distance from the coast, 19 August, 1984 13.50 h.

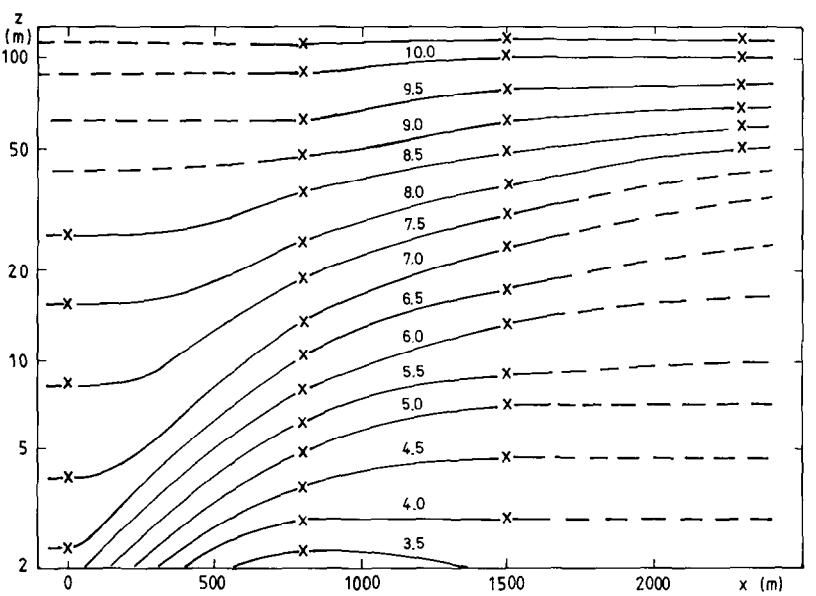

Fig. 5. The observed wind velocity field (m s^{-1}) versus height and distance from the coast, 19 August, 1984 20.45 h.

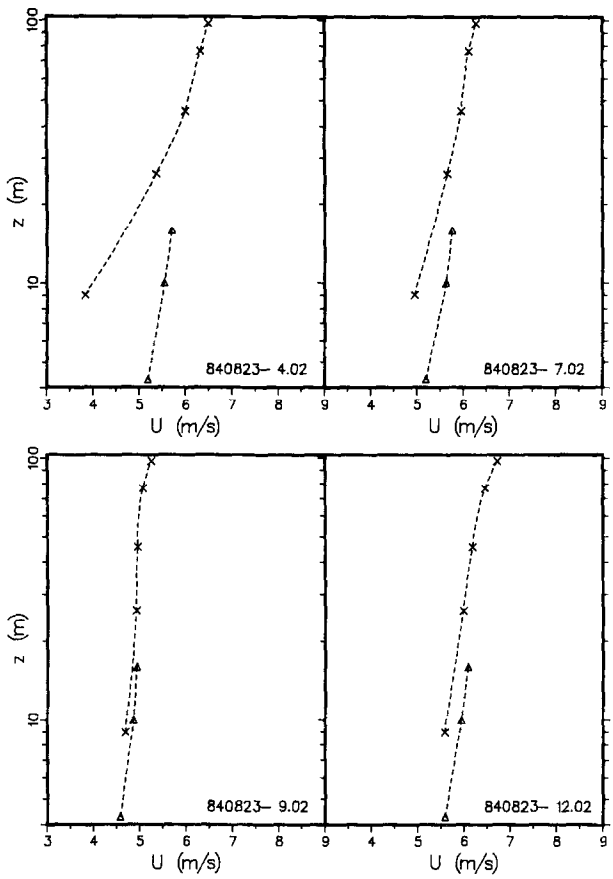

Fig. 6. Observed wind profiles at positions 1 (Δ) and 3 (×).

positions 1 and 3 during a 28-hr period. During the nights, when the surface layer over land was stably stratified, the wind speed decreased markedly inland, while during the daytime, when unstable stratification prevailed over land, the two wind profiles were approximately equal. The reason for this is not obvious, but an explanation may be found when considering the relation between wind profile, surface roughness and thermal stratification. Using the wind model, which will be described in the next section, we may calculate the equilibrium wind profiles for roughness lengths 0.00025 and 0.04 m (representing the sea and the peninsula, respectively) with potential temperature gradients 0.001 K m^{-1} and -0.09 K m^{-1}. These are shown in Figure 8 together with the profile at the distance 1500 m from the coast. An explanation as to why the two equilibrium wind profiles are so close together at heights 5–50 m, in spite of the fact that the roughness length differs by more than two orders of magnitude, may be that the surface friction certainly increases due to the larger roughness, but at the same time, the atmospheric turbulence increases due to enhanced buoyant production. When the

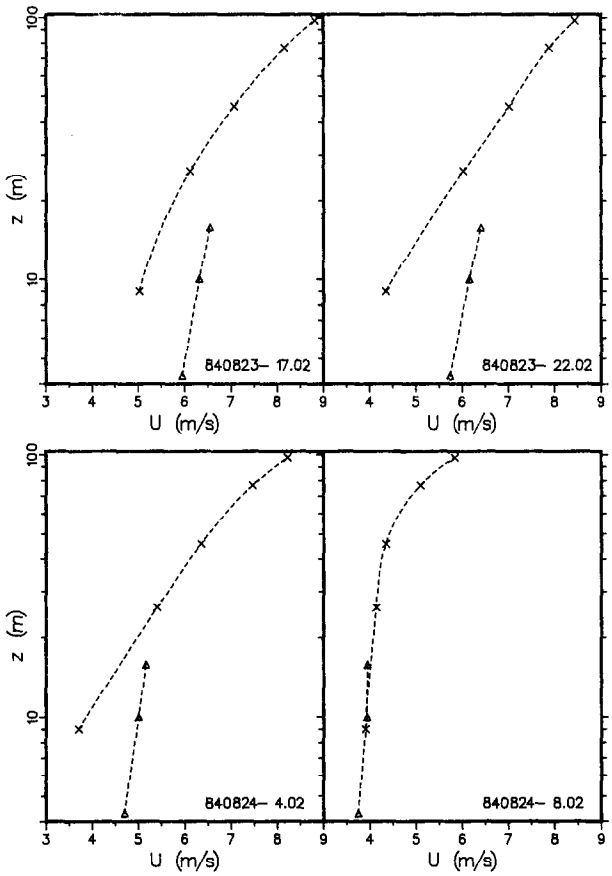

Fig. 7. Observed wind profiles at positions 1 (Δ) and 3 (×).

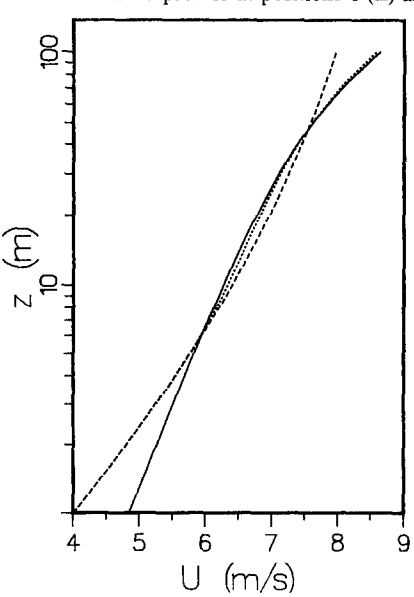

Fig. 8. Modelled wind profiles from 22 August, 1984 8.02 h, illustrating the combined effect of surface roughness and stability; —— equilibrium profile for $z_0 = 0.00025$ m and slightly stable stratification ($1/L = 0.003\ m^{-1}$), – – – – equilibrium profile for $z_0 = 0.04$ m and unstable stratification ($1/L = -0.025\ m^{-1}$), · · · · · · the corresponding profile 1500 m from the shore.

difference in stability between the two surfaces is large, the buoyant production is large enough to compensate for the increased frictional losses of momentum.

An increased wind speed, when passing from a smooth to a rough surface, has been reported by several authors, indicating that other mechanisms than the one proposed above may give rise to an acceleration (or reduced deceleration).

Ogawa and Ohara (1985) report an increased wind speed when passing inland from a coast. They draw the conclusion that the reason for this behaviour in their case was to be found not in the difference in stratification, but rather in the difference in the temperature itself, i.e., the driving force should be a pressure gradient force. But in our case, the temperature difference between land and sea was just a few degrees and no sea breeze circulation was observed.

An acceleration of the wind at a few metres height was also found by Peterson *et al.* (1976) at Risø for distances up to 175 m from the coastline. The reason was to be found in the variation of the elevation of the terrain. The pressure field resulting from the slope (about 1 : 20) was large enough to account for the observed accelerations. In our case, however, the slope of the terrain is only 1 : 300 and might not be expected to be a main reason for the wind speed at $x = 1500$ m not decreasing below the upstream value during daytime conditions. This was tested using the theory for flow above low and gently sloping hills (cf. Smedman and Bergström, 1984). Using data relevant to the Näsudden peninsula, the resulting fractional speed-up ratio, $\Delta U/U$, will only be about 1%. For the profiles presented in Figures 6 and 7, the effect of the terrain slope would thus be less than 0.1 m s^{-1}, i.e., much less than the effects of the difference in roughness and thermal stability.

Bornstein and Johnson (1977) have observed increased wind speed over New York as compared to the surrounding areas. They maintain that the acceleration is due to horizontal pressure gradients, directed inward to the centre of the city, and to the decreased stability of the urban atmosphere. Both effects are associated with the urban heat island. Hunt and Simpson (1982) argue that if the upstream wind profile has a low-level jet, as is not uncommon at night, then the increased turbulence over the urban area would transport the elevated velocity excess downward, thus increasing the velocity closer to the ground.

This latter effect could be of some importance in our case, as a wind maximum was sometimes observed in the region of the subsidence inversion. But we believe that, for our data, the main reason that the wind speed did not decrease inland during daytime conditions with very unstable stratification over land, is to be found in the delicate relation between frictional losses of momentum and the production of turbulent kinetic energy, and consequently turbulent vertical momentum transport and redistribution of horizontal momentum. This is also supported by the model simulations. As the modelled equilibrium surface-layer wind profiles are essentially based upon the well accepted Monin–Obukhov similarity theory, we see (cf. Figure 8) that, at least in horizontally homogeneous conditions, thermal differences could well cancel frictional differences, without taking into account horizontal pressure gradients or low-level jets. It seems reasonable that this is also true in the coastal region.

4. Wind Model Simulations

The wind model which we have used is described in detail by Bergström (1986) and will only be briefly outlined here.

The model is, as mentioned earlier, very simple to use and needs only a minimum of input data. Assuming stationary and horizontally homogeneous conditions, the Monin–Obukhov similarity theory may be used in the surface layer, giving the well known relations:

$$\frac{\partial u}{\partial z} = \frac{u_*}{kz}\,\phi_m(z/L)\,, \tag{1}$$

$$\frac{\partial \theta}{\partial z} = \frac{\theta_*}{kz}\,\phi_h(z/L)\,. \tag{2}$$

Above this layer, a K-model of the Ekman–Taylor type is used; thus the momentum equations may be written

$$f(v_g - v) = K\,\frac{\partial^2 u}{\partial z^2}\,, \tag{3}$$

$$f(u - u_g) = K\,\frac{\partial^2 v}{\partial z^2}\,, \tag{4}$$

where the eddy diffusivity K is kept constant, equal to its value at the top of the surface layer. The height of the surface layer is determined by limiting the variations of the vertical momentum flux ($-\overline{u'w'}$) within this layer. The inherent horizontal inhomogeneity associated with IBL studies, is overcome by using a parameterized submodel. Downwind of the surface discontinuity, the wind field is estimated through the relation (cf. Bergström, 1986)

$$U(x, z) = \lambda(x, z)\,[U(\infty, z) - U(0, z)] + U(0, z)\,, \tag{5}$$

where the parameter $\lambda(x, z)$ has been determined from simulations with Enger's (1985) two-dimensional higher-order closure model. As was shown in Bergström (1986), the dependence of $\lambda(x, z)$ upon distance from the discontinuity (x) and height (z) is very much greater than the influence from thermal stability, surface roughness or pressure gradients. Thus, as a first approximation, λ has been taken to depend only upon x and z.

The input data needed to run the model are:

- Roughness length for the two surfaces (0.00025 and 0.04 m, respectively).
- Upstream wind at one level (10 m).
- Upstream and downstream temperature at two levels.

The values given within parentheses are the ones valid for the Näsudden site and which we have used in this study. The upwind data were taken from the Österudd tower (position 1, Figure 1). Most of the time, the upstream conditions were slightly unstable

according to the measurements. In a few cases, however, the observations showed stable stratification, but this is, for several reasons, not believed to be correct. Among other things, an analysis of the sea surface temperature southwest of Gotland, made by SMHI (the Swedish Meteorological and Hydrological Institute), shows a rise in water temperature when approaching the island. Also, the temperature measurements at position 1 were affected by electronical malfunctioning. Thus we have tried to run the model both with neutral and slightly unstable stratification in those cases also. Both runs gave very similar results, and the upstream wind profile agreed much better with the observations than if a stable upwind stratification was used. We have consequently put the upwind temperature gradient equal to $-0.001\ \mathrm{K\,m^{-1}}$ in those cases when the profile at Österudd gave stable stratification.

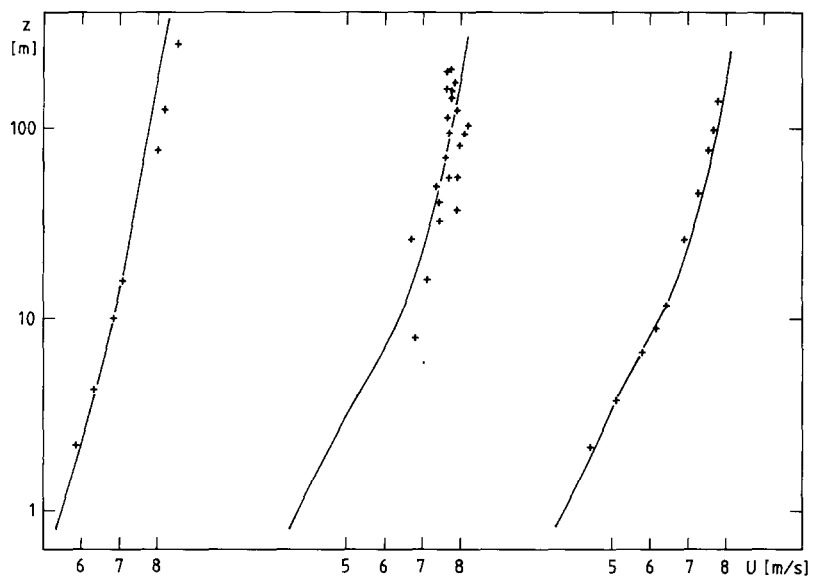

Fig. 9. Wind velocity profiles at positions 1–3 on 19 August, 1984 13.50 h. The full lines give the modelled profiles, the markers give the observed ones.

In Figure 9, the model wind profiles at positions 1–3 are plotted together with the observed profiles from 19 August 13.50 h. The model agrees quite well with the observations. It is also interesting to see that although quite different techniques have been used to measure the wind speed, all give very similar results at heights where it could be expected that there should be no difference in wind velocity.

A summary of the wind model tests is given in Table II. For distances up to 1500 m, the model gives quite satisfactory results, the mean relative error being just about 2% with a standard deviation of 2–10%. The agreement with the sodar-measurements (x = 2300 m) is somewhat less. But, as discussed in Section 3, we have good reasons to believe that the sodar-data are of lower quality.

TABLE II

Results from the wind model test giving distance from the coast, x, mean value and standard deviation of $(u_m - u_0)/u_0$ at some heights where u_m and u_0 are the modelled and observed wind speeds, respectively. The numbers of observations are given in parentheses.

x (m)	Height (m)			
	20	50	100	200
0	0.012 ± 0.017 (20)	−0.004 ± 0.049 (7)	−0.003 ± 0.043 (7)	−0.008 ± 0.088 (6)
800	0.016 ± 0.080 (16)	0.032 ± 0.096 (20)	0.019 ± 0.070 (20)	0.024 ± 0.056 (20)
1500	0.026 ± 0.070 (20)	0.024 ± 0.064 (20)	0.017 ± 0.062 (20)	–
2300	–	0.085 ± 0.094 (18)	0.051 ± 0.103 (18)	0.075 ± 0.144 (13)

We may thus conclude that this relatively simple wind model may be used to estimate the inland wind profile, at least for distances up to some kilometres from the coast and for the rather smooth areas which are of interest for wind turbine siting. Compare also with Bergström (1986), where the model results showed good agreement with observations also at a distance 14 km from the coast.

To test how the wind modification downwind of the coast depends on stability, the model has been run for three different thermal stratifications, upwind as well as downwind, giving altogether nine cases shown in figures 10–12. The stability parameter, z/L, was chosen to be -0.5, 0, and 0.5 at 10 m height, for the unstable, neutral and stable cases, respectively. All runs were made with a geostrophic wind of 10 m s^{-1} and the roughness length was taken to be 0.00025 m upstream and 0.04 m downstream.

With unstable stratification upstream (Figure 10), the reduction in wind speed 1.5 km distance from the shoreline is at 10 m height 12, 22, and 33% for unstable, neutral and stable inland stratification, respectively. The corresponding figures at 75 m are 1.5, 2.5, and -0.5%, i.e., with stable stratification over land, the model gives a slight acceleration of the wind at 75 m.

The simulations with neutral stratification over the sea are presented in Figure 11. Here the wind speed reductions at the distance 1.5 km are at 10 m 2.3, 16, and 28% for the three inland stabilities, while the reductions at 75 m height are <1, 1, and -1.5%.

From the observations shown in Figures 4 and 5, we get reductions of about 7% (daytime) and 26% (night-time) at 10 m height. As the upwind conditions were near neutral, this is in good agreement with the modelled values. At 75 m height, the observed reductions are, however, about 5% in both cases, which is somewhat more than the model gives.

Finally the results from the simulations with stable upstream stratification are

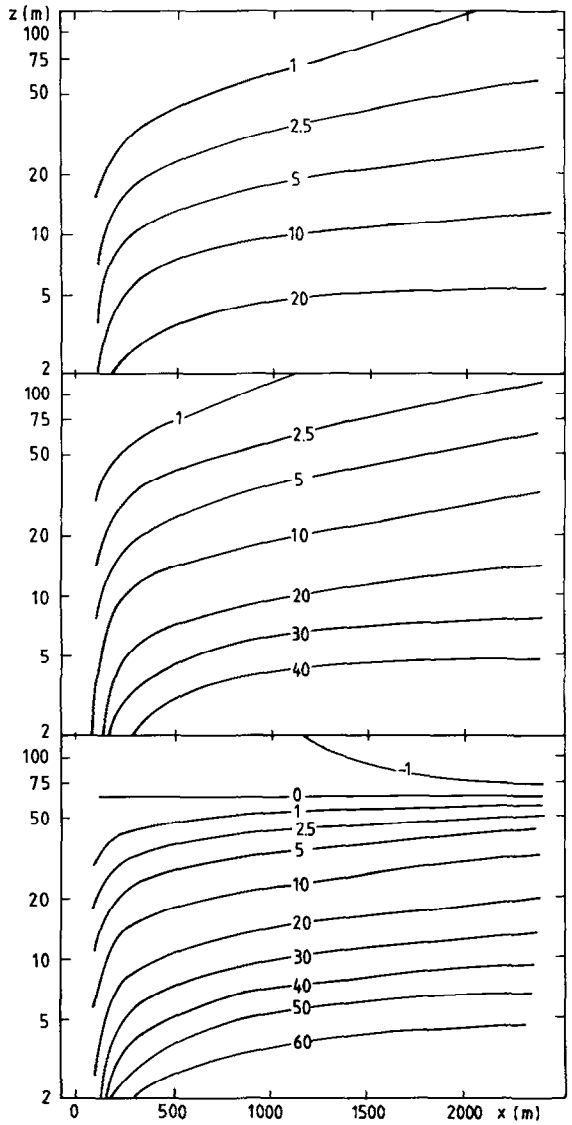

Fig. 10. Isolines of $(U_0 - U_x)/U_0$ (%), calculated with the wind model, versus height and distance from the coast. U_0 is the upstream wind speed and U_x is the wind speed at the distance x. The geostrophic wind is 10 m s^{-1}. Unstable upwind stratification and, from the top, unstable, neutral and stable stratification over land.

presented in Figure 12. Having unstable stratification over land, the model gives an increased wind speed at the 10 m level of about 12% 1.5 km from the coast. This may seem a bit surprising, but as we saw earlier in Section 3, there are occasions when the observed data show no wind speed reduction between positions 1 and 3. There are even a few cases with rather low wind speed (3–4 m s^{-1} at 10 m) when the observations give

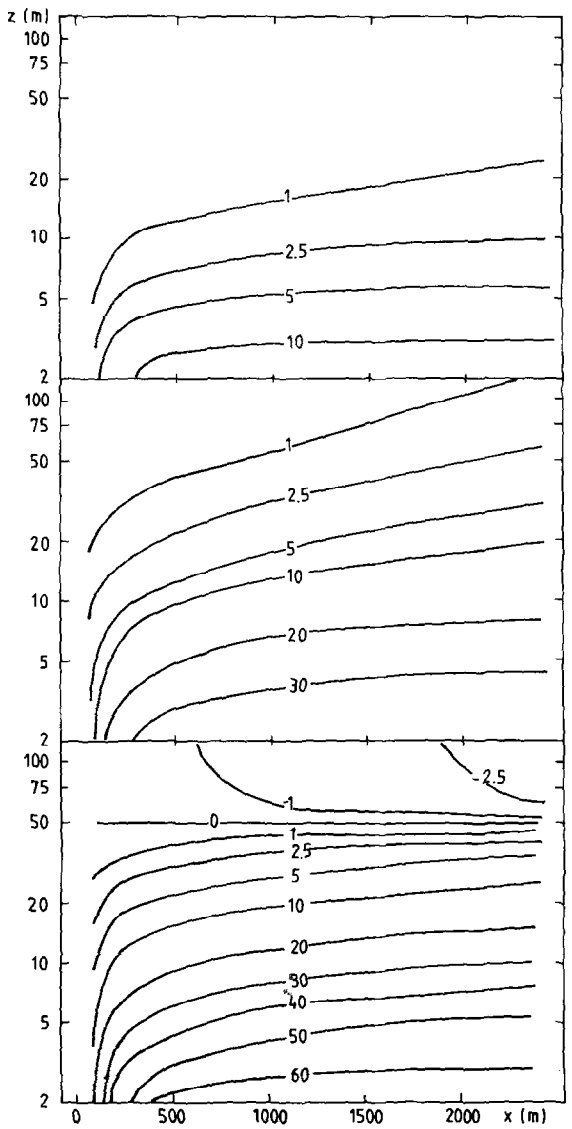

Fig. 11. Same as Figure 10, but neutral upwind stratification.

a somewhat higher (~ 0.5 m s^{-1}) wind speed inland at the heights 10–20 m. All these observations are from situations with very unstable stratification over the land, and consequently very large differences in stability between the downstream and upstream surface (neutral or slightly unstable over the sea). Thus the increase of about 12% given by the model for the 'stable to unstable' simulation does not seem unreasonable. At the 75 m level, the model gives for the same run a decrease in wind speed of about 1.5% 1.5 km from the shoreline. For neutral and stable stratification inland, the corresponding

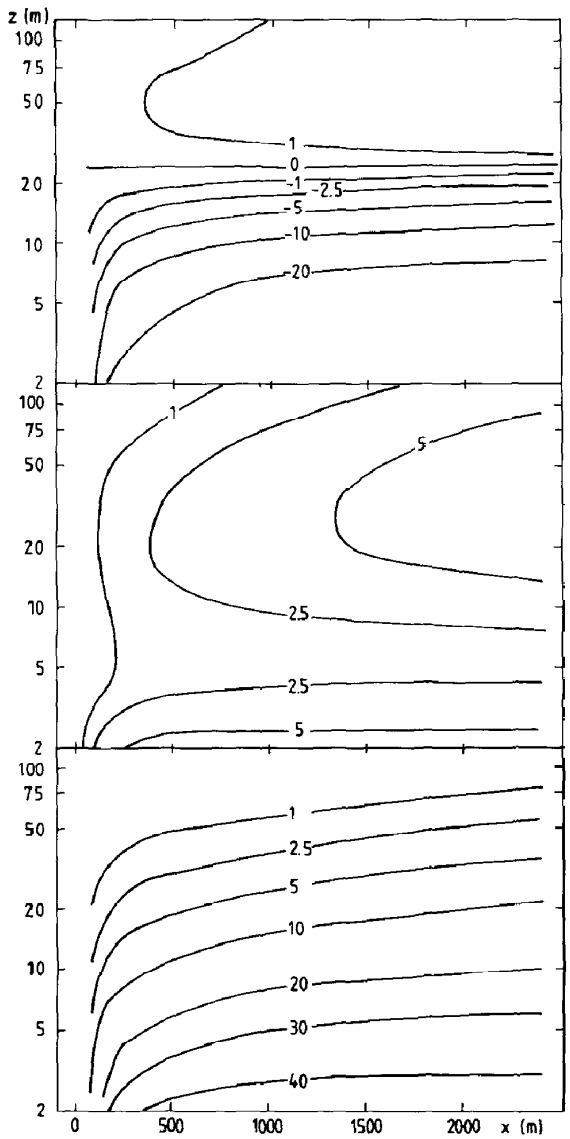

Fig. 12. Same as Figure 10, but stable upwind stratification.

reductions are about 4 and $<1\%$, respectively, while the reductions at 10 m are 3 and 18%.

5. The IBL Height

Not only is the inland decrease in wind speed of importance in wind energy applications, but also the height of the IBL. If this height were at hub-height, the wind turbine would experience not only an increased mean wind speed shear, but also the blades would pass

through two layers having very different degrees of turbulence. As may be seen in Table I, σ_u often decreases by a factor 2 or 3 from the 11 to the 135 m level when the wind direction is from the sea.

As it is rather difficult to use tethered balloon data to determine the IBL height exactly (cf. above regarding this measurement technique), we have only used the tower data from positions 1 and 3 (cf. Figure 1). Then it is no longer necessary to confine ourselves to periods having measurements with the tethered balloon, the amount of data available within the wind direction interval accepted for IBL studies (200–230°) was increased to 91 hours. All these profiles were plotted, as shown in Figure 13, and the IBL heights were determined by extrapolating the profile at Österudd upward until it coincided with the profile at position 3. As seen from the figure, it is then rather easy to get a reasonable estimate of z_{IBL}. This was possible in the majority of cases studied, but as was shown in Figures 6 and 7, there are some periods when it is impossible to determine z_{IBL} from the wind profiles alone.

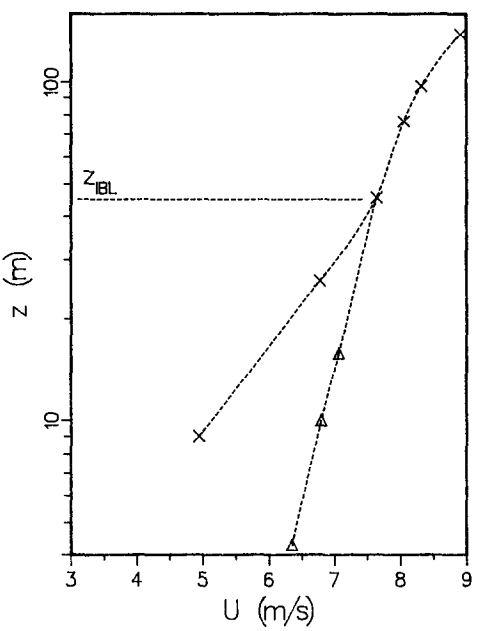

Fig. 13. Observed wind profiles at positions 1 (Δ) and 3 (×) on 22 August, 1984 22.02 h. The figure illustrates how z_{IBL} has been determined.

Next we would like to model the IBL height growth. Many such models have been given in the literature, e.g., Elliott (1958), Miyake (1965), Pasquill (1972), Smedman and Högström (1978), Wood (1981), Højstrup (1981). We shall also try to determine z_{IBL} using the wind model discussed above.

An IBL-height model should be able to take into account both surface roughness and thermal stratification. The roughness dependence may of course not be studied with our

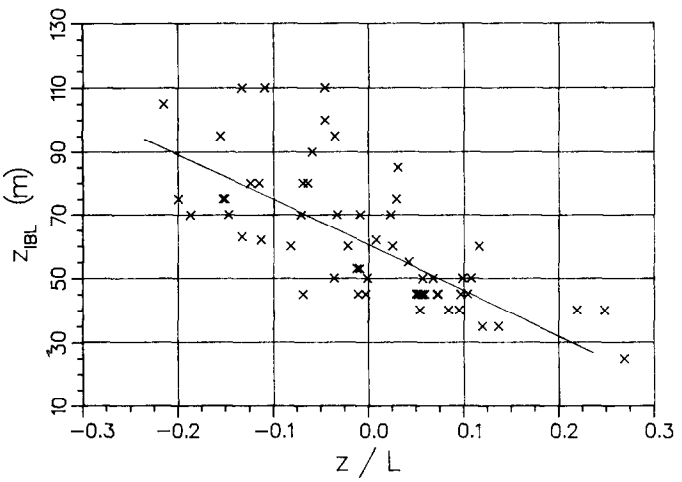

Fig. 14. The measured height of the IBL versus stability at position 3, 11 m level. The line is the result of the linear regression $z_{IBL} = 61-141z/L$.

data, as they are all from the same site, but the importance of the stability of the IBL is illustrated in Figure 14, where the observed z_{IBL}-values are plotted versus the stability parameter z/L as measured by the turbulence instrument at the 11 m level at position 3, taken to be representative for the peninsula. Observations where z_{IBL} could not be determined from the wind profile are then excluded. There is, as expected, an apparent dependence upon stability, although the scatter is quite large. The IBL height at the distance 1500 m from the coast increases from about 40 m for stable stratification ($z/L = 0.15$) to about 80 m during unstable conditions ($z/L = -0.15$). Linear regression yields $z_{IBL} = 61-141z/L$, with a correlation coefficient of 0.71. The slope of the IBL is then consequently 1 : 25 as a mean for neutral conditions. A possible influence on z_{IBL} from the upstream thermal conditions may, however, not be investigated from our data, as the conditions over the sea did not vary much during the experiment, cf. above.

Using the wind model, the IBL height was determined from the following equation:

$$\frac{U(0, z_{IBL}) - U(x, z_{IBL})}{U(0, z_{IBL})} = A\,, \tag{6}$$

where

$U(0, z_{IBL})$ = upstream wind speed at height z_{IBL}

$U(x, z_{IBL})$ = downstream wind speed at height z_{IBL}

A = a constant.

The best agreement between observed and calculated values of z_{IBL} was obtained with $A = 2.5\%$. As illustrated in Figure 15, the model gives satisfactory estimates of the IBL when the downwind stratification is stable or near neutral. With unstable downwind conditions, this type of model gives far too low values. This is due to the reduced deceleration of the wind speed over land, as was discussed in Section 3.

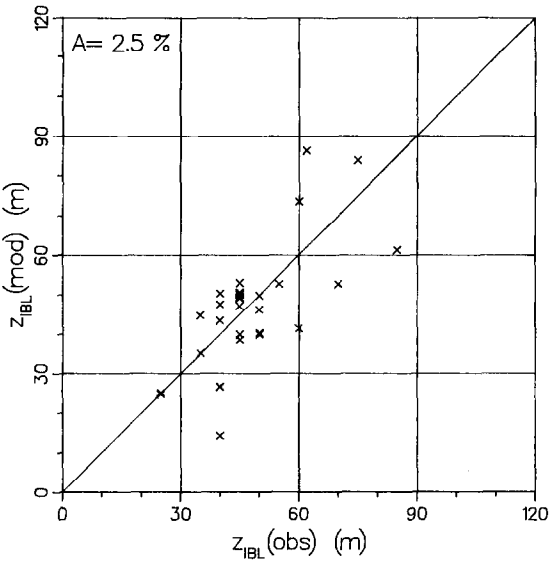

Fig. 15. Modelled IBL heights versus observed ones. The wind model has been used and z_{IBL} was taken to be the level at which the constant A in Equation (5) was set equal to 2.5%.

Keeping the downwind stratification stable, the wind model was used to study the influence of varying upwind stability on the IBL-height. Using $1/L = 0.01\ \mathrm{m}^{-1}$ downstream and $x = 1500$ m, we get the following results:

$1/L$ upstream:	-0.02	-0.01	0	0.01	0.02,
z_{IBL}:	63	61	53	51	60.

There is, during these rather moderately diabatic conditions, no greater dependence of z_{IBL} on the upwind conditions, at least not according to the model. But this result indicates that the upwind conditions are less important to the IBL growth than the downwind conditions, cf., Figure 14.

As it is sometimes not possible to use the wind model to describe the IBL-height when the downstream stratification is unstable and the upstream conditions are stable or neutral, we shall try to use the simple model proposed by Smedman and Högström (1978), where the height of the IBL, z_{IBL}, is determined through a relation of the type

$$z_{IBL} = a \cdot x^b, \tag{7}$$

where a and b are functions of both roughness length and stability. Using the values of a and b recommended by Smedman and Högström (1978) will, however, give IBL-heights that are much too high compared to observed ones over a large range in z/L. In Figure 16, the IBL-heights from the Smedman–Högström formula are shown together with the heights calculated with our new b-value; see below. As originally reported by Pasquill (1972), the parameter a varies much more with surface roughness

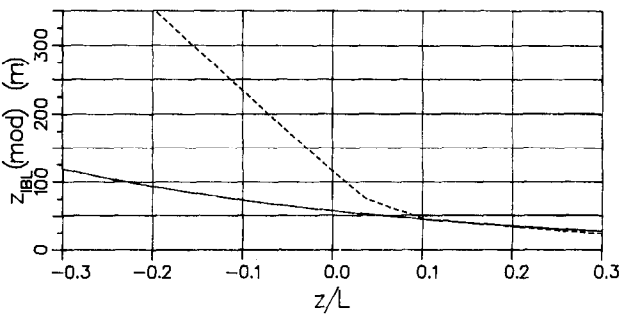

Fig. 16. The IBL height versus stability, calculated from Equation (6) using the parameters a and b given by Smedman and Högström (1978) (dashed line) and determined from our data (full line).

than with stability; thus we choose to keep this constant while we take b to be a function of stability. Looking at Table I in Smedman–Högström (1978), we see that this procedure should be quite accurate for small z_0, such as our value of 0.04 m. Keeping the value of a that was proposed by Smedman and Högström and using the data presented in Figure 14 to determine the relationship for b, we get:

$$z_{IBL} = 0.2x^{(0.78 - 0.33z/L)}. \tag{8}$$

In the neutral case, this implies that b in Equation (7) is equal to 0.78 which is very close to the commonly proposed value of 0.8, given by e.g., Elliott (1958) and Wood (1981). The IBL-heights, calculated from Equation (7), as a function of z/L are shown in Figure 16. The modelled IBL-heights are compared with the observed ones in Figure 17. The scatter is not larger than might be expected when comparing with Figure 14.

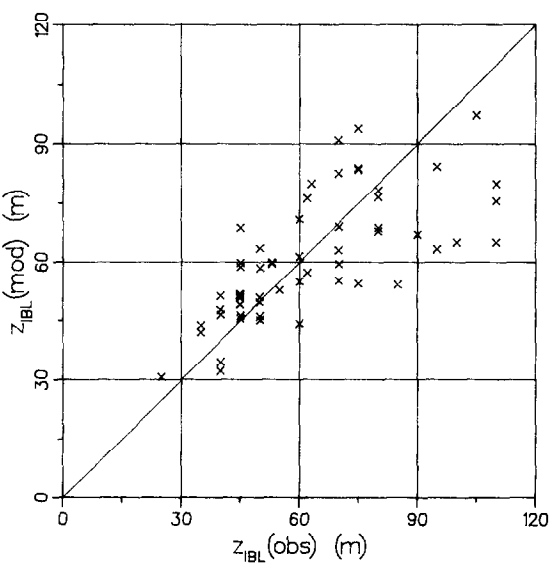

Fig. 17. Modelled IBL heights (Equation (7)) versus observed ones.

8. Summary and Conclusions

Analysis of a rather comprehensive amount of data from a coastal site shows that it is not always possible to discern the IBL which is formed downstream of the coastline, using wind profile data alone. Despite increased surface roughness, there is a not negligible amount of data for which the wind speed at 10–20 m height is very similar over the sea as at 1.5 km inland. There are even cases when the wind is somewhat higher at the inland position than at the coastline. The cause of this behaviour is not obvious, but as the slope of the terrain is very small (1 : 300) and the difference in air temperature over sea and land is only a few degrees, it does not seem likely that either of these factors is important. Instead the phenomenon is probably caused by vertical redistribution of momentum by the enhanced turbulence over land. When the air flow passes the coastline, turbulence is produced partly as a result of increased surface roughness, but mainly (during unstable conditions) it is the buoyant production term which increases the vertical momentum transport so that it compensates for the larger frictional losses of momentum which are experienced over land.

This is supported by simulations with a simple wind model. The model has been tested against observations, and the mean difference between model predictions and the observations was found to be 2% with a standard deviation of 2–10%. Thus, in spite of its simplicity, the wind model may be used to simulate the transformation of the wind profile in a coastal region with flow from the sea. Comparing the calculated surface-layer wind profile over the sea and over the land (Figure 8), we see that the model may indeed give the observed acceleration of the wind in the height interval 5–50 m, as a result of increased turbulent momentum transport.

The height of the IBL was determined 1.5 km inland by comparing the wind profiles measured there with those observed at the coast (excluding the cases with no or very small inland decrease of the wind). A distinct stability dependence of the IBL heights could be seen, cf. Figure 14, where the stability parameter z/L was calculated using measured turbulent fluxes at 11 m. Because the upstream conditions over the sea were approximately the same for all data, any influence from the stability over the sea could not be investigated. But a model simulation indicates that the upwind stratification is less important than the downwind conditions.

We have thus shown that rather simple models may be used to study the modification of the wind speed and the height of the IBL in a coastal region with onshore winds. With knowledge of the climatological statistics of wind and stability, the models may be used as tools to estimate the climatology of wind and IBL height at different distances from a coast, which is of great interest when locating wind turbines.

Acknowledgement

We are grateful to all who participated in and made the NIBWAK experiment possible. The investigation was sponsored by the National Energy Administration in Sweden.

References

Alexandersson, H. and Bergström, H.: 1979, *Evaluation of Double Theodolite Pibal Tracking Data.* Report No. 56. Department of Meteorology, Uppsala University, 72 pp.

André, J. C., de Moor, G., Lacarrère, P., Therry, G., and du Vachat, R.: 1978, 'Modeling the 24-hour Evolution of the Mean and Turbulent Structure of the Planetary Boundary Layer', *J. Atm. Sci.* **35**, 1861–1883.

Bergström, H.: 1986, 'A Simplified Boundary Layer Wind Model for Practical Application', *J. Clim. Appl. Meteorol.* **25**, No. 6, 813–824.

Bornstein, R. D. and Johnson, D. S.: 1977, 'Urban-Rural Wind Velocity Differences', *Atmos. Environ.* **11**, 597–604.

Bradley, E. F.: 1968, 'A Micrometeorological Study of Velocity Profiles and Surface Drag in the Region Modified by a Change in Surface Roughness', *Quart. J. Roy. Meteorol. Soc.* **94**, 361–379.

Elliott, W. P.: 1958, 'The Growth of the Atmospheric Internal Boundary Layer', *Trans. Amer. Geophys. Union* **39**, No. 6, 1048–1054.

Enger, L.: 1986, 'A Higher Order Closure Model Applied to Dispersion in a Convective PBL', *Atmos. Environ.* **20**, No. 5, 879–894.

Gamo, M., Yamamoto, S., and Yokoyama, O.: 1982, 'Airborne Measurements of the Free Convective Internal Boundary Layer During the Sea Breeze', *J. Meteorol. Soc. Japan* **60**, 1284–1298.

Hunt, J. C. R. and Simpson, J. E.: 1982, 'Atmospheric Boundary Layers over Non-Homogeneous Terrain', in E. J. Plate (ed.), *Engineering Meteorology*, Chapter 7, pp. 269–318.

Högström, U.: 1982, 'A Critical Evaluation of the Aerodynamical Error of a Turbulence Instrument', *J. Appl. Meteorol.* **21**, 1838–1844.

Högström, U., Enger, L., and Knudsen, E.: 1980, *A Complete System for Probing the Detailed Structure of Atmospheric Boundary Layer Flow*, Report No. 60, Department of Meteorology, Uppsala University, 47 pp.

Högström, U., Taesler, R., Karlsson, S., Enger, L., and Smedman, A.: 1978, 'The Uppsala Urban Meteorology Project', *Boundary-Layer Meteorol.* **15**, 69–80.

Højstrup, J.: 1981, 'A Simple Model for the Adjustment of Velocity Spectra in Unstable Conditions Downstream of an Abrupt Change in Roughness and Heat Flux', *Boundary-Layer Meteorol.* **21**, 341–356.

Mellor, G. L. and Yamada, T.: 1974, 'A Hierarchy of Turbulence Closure Models for Planetary Boundary Layers', *J. Atm. Sci.* **31**, 1791–1806.

Miyake, M.: 1965, *Transformation of the Atmospheric Boundary Layer over Inhomogeneous Surfaces*, Scientific Report, Office of Naval Research, Contract 477(24) (NR 307–252).

Ogawa, Y. and Ohara, T.: 1985, 'The Turbulent Structure of the Internal Boundary Layer Near the Shore (Part 1: Case Study)', *Boundary-Layer Meteorol.* **31**, 369–384.

Pasquill, F.: 1972, 'Some Aspects of Boundary Layer Description', *Quart. J. Roy. Meteorol. Soc.* **98**, 469–494.

Peterson, E. W.: 1969, 'Modification of Mean Flow and Turbulent Energy by a Change in Surface Roughness under Conditions of Neutral Stability', *Quart. J. Roy. Meteorol. Soc.* **95**, 561–575.

Peterson, E. W., Kristensen, L., and Chang-Chun Su: 1976, 'Some Observations and Analysis of Wind over Non-uniform Terrain', *Quart. J. Roy. Meteorol. Soc.* **102**, 857–869.

Raynor, G., Sethuraman, S., and Brown, R.: 1979, 'Formation and Characteristics of Coastal Internal Boundary Layers during Onshore Flows', *Boundary-Layer Meteorol.* **16**, 487–514.

Salomonsson, S.: 1982, *Doppler Sodar for Wind Measurements*, Report No. FL8–2 Swedish Space Corporation.

Smedman, A. and Bergström, H.: 1984, 'Flow Characteristics Above a Very Low and Gently Sloping Hill', *Boundary-Layer Meteorol.* **29**, 21–37.

Smedman, A. and Högström, U.: 1978, 'A Practical Method for Determining Wind Frequency Distributions for the Lowest 200 Meters from Routine Meteorological Data', *J. Appl. Meteorol.* **7**, 942–954.

Smedman, A. and Högström, U.: 1983, 'Turbulent Characteristics of a Shallow Convective Internal Boundary Layer', *Boundary-Layer Meteorol.* **25**, 271–287.

Smedman, A. and Melas, D.: 1986, *The Öresund Experiment. Description of Measurements Performed by MIUU*, Report No. 84, Department of Meteorology, Uppsala University, 45 pp.

Smedman, A. and Lundin, K.: 1987, *Psychrometer Systems for Measurements of Temperature and Humidity Profiles in the Atmospheric Boundary Layer*, Report No. 76, Department of Meteorology, Uppsala University.

Wood, D. M.: 1981, 'Internal Boundary Layer Growth Following a Step Change in Surface Roughness', *Boundary-Layer Meteorol.* **22**, 241–244.